Journal of Hydraulic Structures
J. Hydraul. Struct., 2024;11(3):1-13
DOI: 10.22055/jhs.2024.47610.1315

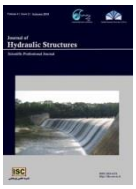

OPEN ACCESS

Non-homogeneous embankment dams overtopping breach: Experimental study of flow level variations and reservoir sediment movement

Mahdi Ebrahimi [1]
Mirali Mohammadi [*1]
Sajad Bijanvand [2]

Abstract

The overtopping phenomenon is the most probable reason for embankment dams' failure. It includes an intricate process; hence its experimental investigation is a remarkable subject. In current research work, two experiments have been conducted at the hydraulics laboratory of the Iranian Energy Ministry Water Research Institute. The changes of reservoir water level, and downstream sedimentary flow level were measured in the first experiment. The first experiment results represented in three stages, i.e., initiation, development, and termination. In case of initiation, the water level rise observed 6% in reservoir. In the development stage, the variation rate of reservoir water level was two times of the termination stage. In the second experiment, the reservoir sediment modeling was performed. When the second experiment finished, about 10% of reservoir sediment was transported downstream. Besides that, the average eroded material thickness was increased, it proved the effect of the reservoir sediment movement. This article comprises calculation of the volume and mass of the eroded material in two practical experiments. The current research helps researchers to achieve the new insight on breach results of embankment dams.

Keywords: Dam breach, Flow level measurement, Physical model, Sedimentation pattern.

Received: 09 August 2024; Accepted: 21 October 2024

[*] E-mail: m.mohammadi@urmia.ac.ir **(Corresponding Author)**
[1] Department of Civil Engineering, Faculty of Engineering, Urmia University, Urmia, Iran.
[2] Department of Civil Engineering, Faculty of Engineering, Imam Ali University, Tehran, Iran.

Notations

T	Time [s]
ϕ	Internal friction angle parameter [degree]
C	Cohesion parameter [$\frac{KN}{m^2}$]
R	Compaction percentage [-]
γ_d	Dry specific weight [kg/m^3]
γ_{dmax}	$Maximum$ dry specific weight [kg/m^3]
SM	Silty sand [-]
CL	Low plasticity clay [-]
H_u	reservoir water level [cm]
H_d	Downstream sedimentary flow level [cm]
H	Maximum magnitudes of downstream sedimentary flow level [cm]

1. Introduction

The experimental analysis of non-homogeneous embankment dam overtopping failure is crucial for several reasons: the prevalence of non-homogeneous embankment dams worldwide; overtopping being the most frequent cause of embankment dam failure [1]; the presence of an impermeable core, which complicates failure analysis compared to homogeneous dams; and the scarcity of adequate laboratory data to assess hydraulic failure impacts. Overtopping occurs when water flows over the dam crest, leading to erosion of the dam structure. Key causes include the absence of a sufficient spillway, reduced reservoir capacity due to sediment buildup, and dam settlement [2]. This phenomenon carries significant implications for life safety, financial loss, and environmental management. Additionally, sediment transport during dam failure is a critical concern, necessitating an understanding of sediment movement patterns and deposition following the dam's end-of-life phase or removal. The flow resulting from embankment dam breach is highly unsteady and variable, characterized as a muddy flow due to dam body erosion and sediment mobilization. Typically, this phenomenon is studied using comparative, regression, semi-physical, and physical models. Non-experimental modeling involves simplifications that can significantly impact the accuracy of results, given the numerous factors influencing embankment dam overtopping failure. Analyzing reservoir water level changes, downstream sediment flow variations, and dam material transport is essential for developing a comprehensive strategy to manage the destructive outcomes of the breach process.

Several experts have conducted investigations to determine the overtopping breach results of embankment dams. In the IMPACT project [3], two large-scale non-homogeneous models were constructed, with significant results including the study of the breach process and the development of numerical models. Pugh [4] proposed a pattern for fuse plug spillways material grain size distribution and studied their breach procedure. Hanson et al. described the JET test to estimate the erodibility coefficient and assess embankment dams' performance during overtopping flow [5]. Al-Riffai focused on the geotechnical and hydraulic aspects of the embankment dam breach mechanism by conducting several experiments [6]. Froehlich presented two mathematical models to predict maximum discharge by measuring embankment dam breach outflow events, which offered more accurate predictions [7]. Abdellatif and El-Ghorab examined two small-scale experiments to study the scale effects on the embankment dam breach process, concluding that the erodibility and breach rate were nearly the same in both experiments [8]. Novel sediment transport equations were developed for modeling homogeneous embankment dam breach on steep bed slopes [9]. Saberi developed a breach hydrograph using numerical

methods, concluding that for channel bed slopes of less than 1%, the Meyer-Peter-Muller equation is the most valid for bed sediment load transport [10]. Researchers at the Energiforsk Institute constructed two laboratory models (1/6 and 1/3 scales) for a real fuse plug, concluding that both models provided a complete picture of dam breach behavior [11]. Sadeghi et al. conducted research on the physical modeling of non-homogeneous embankment dams, finding that as core cohesion increases, the peak discharge and its time of occurrence also increase [12]. Additionally, they found that when core cohesion decreases significantly, the breach formation process becomes similar to that of homogeneous dams. Desta and Belayneh used HEC-RAS to analyze the breach of the Gidabo embankment dam for overtopping failure, calculating the breach parameters, peak outflow, and maximum depth [13]. The effect of riprapping on the failure mechanism of levees was also investigated, with results showing that riprap cover significantly prevented the expansion of the levee breach, delayed erosion, and increased failure time [14]. Taskaya et al. investigated sediment movement resulting from homogeneous dam overtopping breach, revealing that a significant portion of the dam body was carried away by flood flow, with final sedimentation showing non-uniform variation in thickness both longitudinally and transversely [15].

Based on the research background, few studies have focused on the overtopping breach of non-homogeneous embankment dams. Additionally, significant gaps exist in understanding the variations in rerervoir water levels, changes in downstream sediment flow, and the movement of reservoir sediment. This study aims to address these gaps by performing two types of experiments. The first experiment investigates upstream and downstream flow level variations; and the second experiment studies the reservoir sediment movement to downstream region during breach procedure.The results provide new insights for managing the adverse consequences of embankment dams breach.

2. Materials and Methods

2.1. Experimental setup and measurements

Physical modeling was conducted at the Hydraulics Laboratory of the Iranian Energy Ministry Water Research Institute (IEMWRI). To achieve the study's objectives, a cement channel with a width of one meter and a slope of two per thousand was constructed. Five digital cameras were strategically positioned to capture the variations in flow level during the breach process. Due to the high water volume in the reservoir, it was unnecessary to fully drain it to complete the breach process. The initiation and completion times of the breach were recorded by analyzing footage from the cameras placed in front of the two slopes. Initial investigations suggested that the downstream sedimentation length could be estimated at 4 meters. Sedimentation thickness was measured at 140 points using a laser meter, which was attached to a cart positioned on the channel, to determine the difference in channel bed elevation before and after the sedimentation process. The sedimentation plan was then mapped using Surfer software. The inlet flow rate was set at 2.5 liters per second to fill the upstream reservoir, and the reservoir volume at the onset of the breach was 4.7 cubic meters. After each experiment, the recorded video footage was saved on the laboratory computer, and the flow levels were extracted accordingly. Figure 1 illustrates a schematic diagram of the experimental setup.

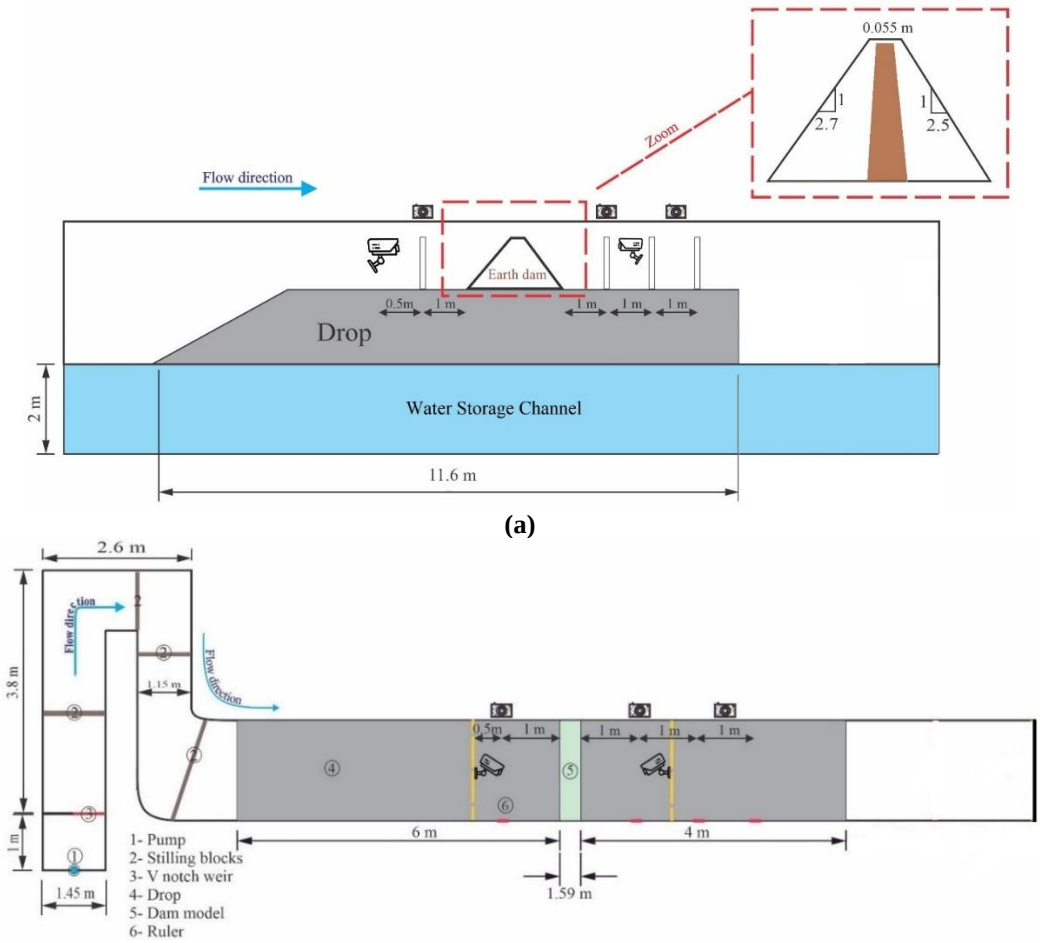

Figure 1. Experimental setup: a) Side view, b) Plan view

2.2. Construction procedure of physical models

The clay and sand samples were examined in the soil mechanics laboratory before the experiments began. Figure 2 illustrates the material gradation curves, where SM and CL represent the gradations of the sand and clay materials, respectively. Additionally, Table 1 and Table 2 detail the core's geometrical and geotechnical properties used in the experiments (refer to ASTM D422-63 [16]; ASTM D698 [17]; ASTM D3080 [18]). The dam's geometry was physically modeled based on a large Iranian non-homogeneous embankment dam, scaled down to a 1/200 geometrical scale [19]. The model adhered to design principles outlined in authoritative sources, such as USBR and USACE [20, 21].

Initially, the impermeable core was constructed in six layers within a 98 cm long wooden mold. Once the compaction process was completed, the mold was rotated 180° to place it in the intended core location, and the mold was then removed (see Figures 3-5). After constructing the impermeable core, the upstream and downstream shells were built. The shell of the physical model was also made in six layers. The compaction of both the core and shell materials was performed using flat hammers, with optimal moisture content of 10% for the core and 9.2% for the shell. Compaction continued until no further volume changes were possible. Eq. (1) was used to calculate the compaction percentage. Table 3 provides the specifications for the shell.

$$R = \frac{\gamma_d}{\gamma_{dmax}} \times 100 \quad (1)$$

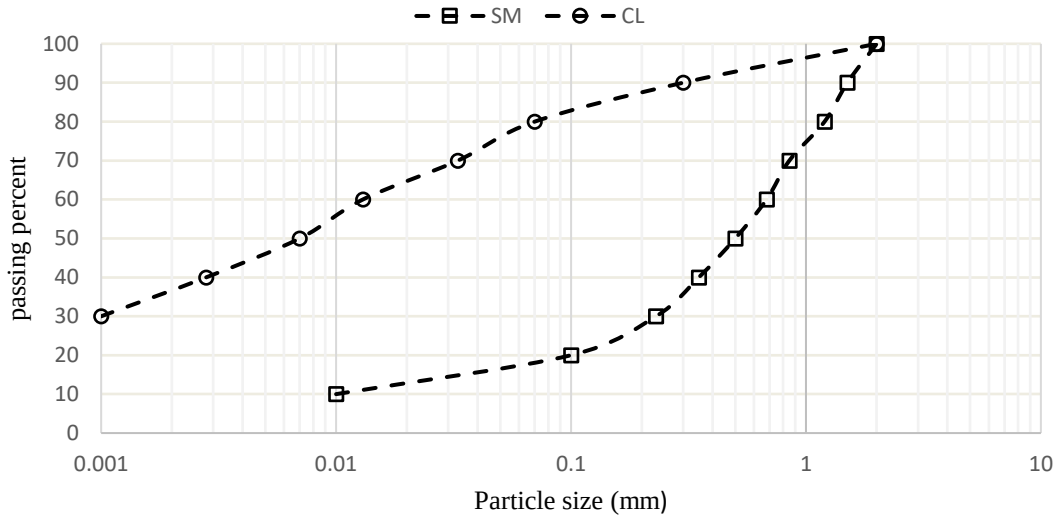

Figure 2. The used material grain size distribution

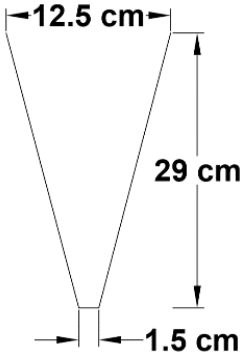

Figure 3. Wooden mold section for impermeable core building

Figure 4. Core compaction in wooden mold

Figure 5. Built core plan

Table 1. Impermeable core geometrical properties

Height (cm)	Top width (cm)	Bottom width (cm)	Upslope (H:V)	Downslope (H: V)
29	1.5	12.5	1:5.2	1:5.2

Table 2. Impermeable core geotechnical properties

ϕ (degree)	C ($\frac{KN}{m^2}$)	ω_{opt} (%)	Combination	classification	weight (kg)	Compaction percent
33	10	10	20% CL & 80% SM	SC	35	90

Table 2. Shell properties

Height (cm)	Top width (cm)	Bottom width (cm)	Upslope (V:H)	Downslope (V:H)	weight (kg)	Compaction percent
29.5	5.5	159	1:2.7	1:2.5	280	65

Before the experiments were conducted, a rectangular groove measuring 10 cm in length and 2.5 cm in depth was carved into the middle of the crest to guide the breach process. Figure 2 presents the gradation curves for the shell and clay materials. For constructing the impermeable core, a mixture consisting of 80% SM (sand) and 20% CL (clay) was selected. Additionally, CL material was used to simulate the reservoir sediment in the second experiment. Table 4 provides the data related to the reservoir sediment. Figure 6 depicts the physical model before the reservoir was filled during the second experiment.

Figure 6. Constructed model in the 2nd experiment

Table 4. Reservoir sediment data

Classification	Length (m)	Thickness (m)	Mass (kg)
CL	1	0.1	125

2.3. The experiments' program

The current research presents the results of two types of experiments, each of which was repeated to ensure consistency in the findings. The first experiment goal is measuring of the reservoir water level variations. Moreover, the mentioned experiment examines the changes of the downstream sedimentary flow level. Furthermore, the purpose of the second experiment is to find out how the reservoir sediment is moved to the downstream. In the second experiment, the upstream and downstream flow level variations have not been measured. In the second experiment, the reservoir sediment was modeled according to 2.2 section explanations. Also, the reservoir sediment was saturated by maintaining the reservoir water level at 26 cm for two hours. The overtopping breach commenced as soon as water reached the downstream slope. At the start of both experiments, the reservoir water level was 27 cm. To determine the dry specific weight of the sediment resulting from the breaching of the non-homogeneous models, four random samples were collected from the bed sediment at the end of the experiments. These samples were then placed in an oven for 24 hours to dry. The dry specific weight was calculated by dividing the dry sample mass by its original volume, and a value of 1450 kg/m³ was determined based on these calculations.

3. Presentation of the results and discussion

3.1. Results for the 1st experiment

Figures 7-9 illustrate the temporal changes in the reservoir water level at a distance of one meter from the heel, the sedimentary flow level at one meter from the toe, and the maximum magnitudes of the downstream sedimentary flow level, respectively. Based on the laboratory findings and the graphs derived from the camera analysis, the breach process of the physical model can be categorized into three significant stages. Figure 10 depicts these breach stages during the first experiment.

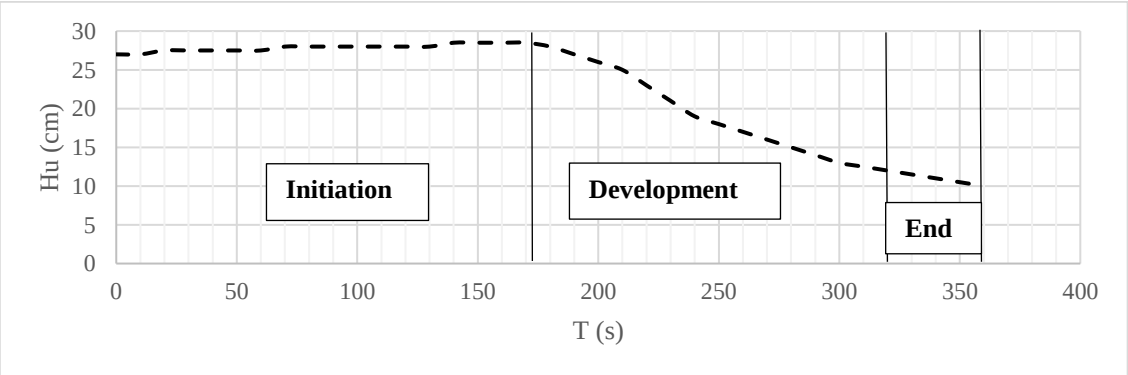

Figure 7. Water level variations at one meter from the heel

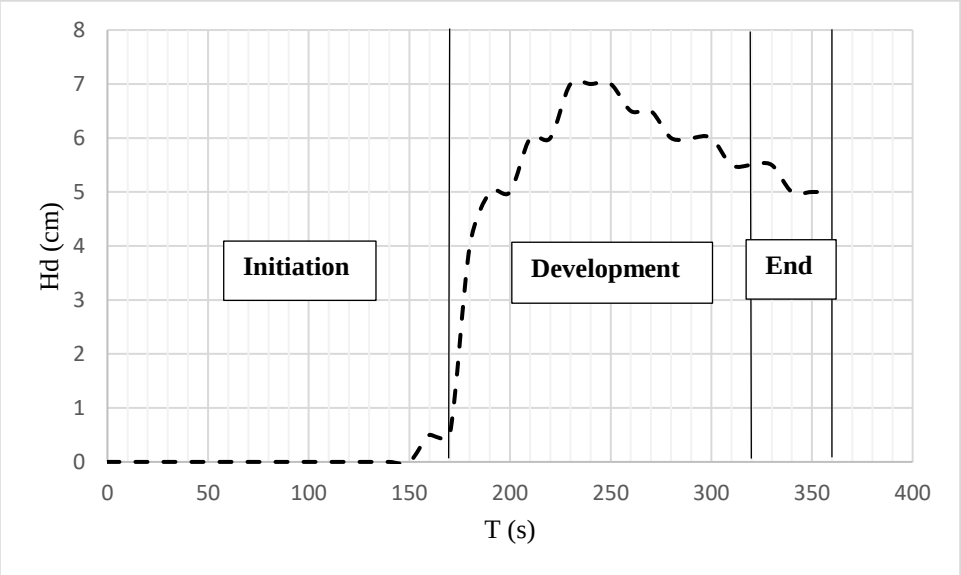

Figure 8. Downstream sedimentary flow level variations at X=1 m

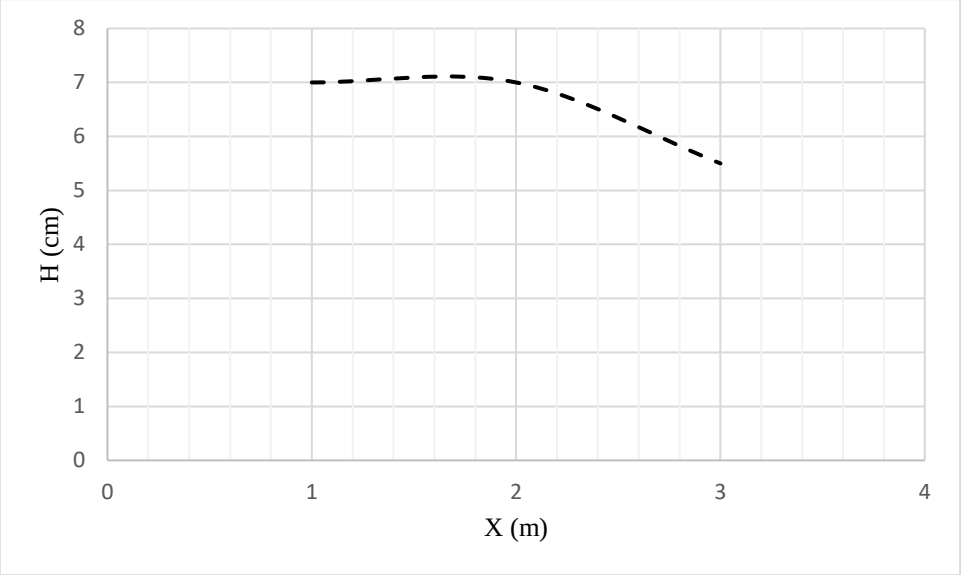

Figure 9. Maximum magnitudes of downstream sedimentary flow level

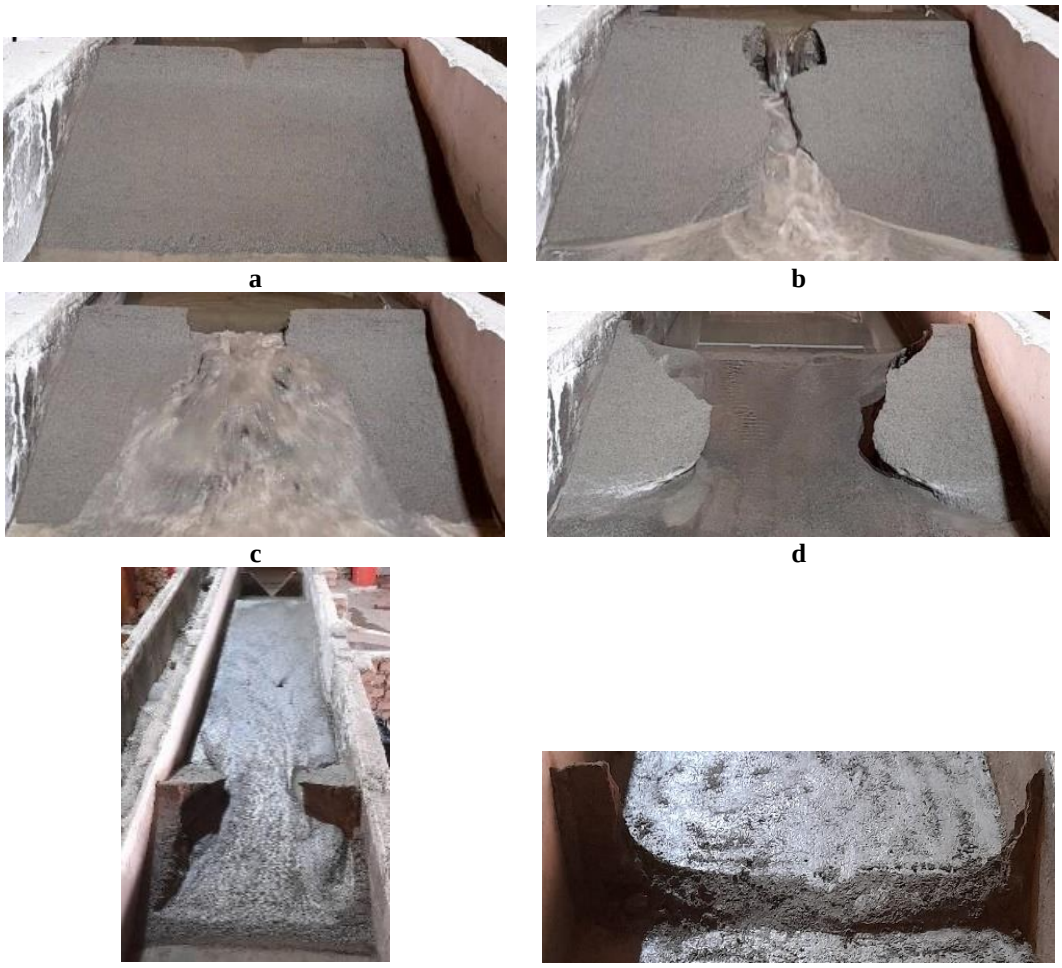

Figure 10. Breach phases: a) Initiation, b) Core breach moment, c) After core breaching, d) End, e) Final status, f) Remaining core after breaching

3.1.1. The first stage: Breach initiation

The first stage begins when water first reaches the downstream slope. During this stage, the breach process follows a straight path along the primary groove in the crest. The dimensions of the groove do not significantly change at this point. The initiation stage was timed at 170 seconds, as observed from the camera positioned in front of the downstream slope, marking the moment when the impermeable core was breached. During this stage, the reservoir water level rose from 27 cm to 28.5 cm, representing a 6% increase. This increase can be attributed to the relative rise in reservoir inflow compared to the breach outflow. By the end of this stage, the downstream ruler, located one meter from the toe, recorded a flow level of 0.5 cm. Observations indicated that the majority of the eroded material accumulated near the toe of the physical model.

3.1.2. The second stage: Breach development

Following the initiation phase, the breach process progresses into the development stage. At the start of this stage, the breach in the impermeable core becomes evident, and the dimensions of the rectangular groove in the crest increase significantly. The duration of the development stage is 150 seconds. During this time, the reservoir water level dropped from 28.5 cm to 12 cm, corresponding to a reduction rate of 0.11 cm/s. The downstream flow level increased from 0.5 cm to 7 cm before settling at 5.5 cm. The maximum flow levels recorded by the three downstream rulers were 7 cm, 7 cm, and 5.5 cm, respectively. According to the experimental findings, the primary sedimentation pattern is formed during this stage.

3.1.3. The third stage: Breach end

The final stage of the breach process lasts for 40 seconds. During this stage, only minor changes in the sedimentation pattern were observed. The reservoir water level decreased from 12 cm to 10 cm, corresponding to a reduction rate of 0.05 cm/s. Additionally, the sedimentary flow level at a distance of 1 (x = 1 m) meter from the toe decreased slightly from 5.5 cm to 5 cm.

3.2. Results for the 2nd experiment

Figure 11 shows the movement of reservoir sediment; and Figure 12 reveals the channel final status after the breach procedure.

Figure 13. Reservoir sediment movement

Figure 14. Final status after the 2nd experiment

3.3. Comparison of sedimentation patterns

Figure 13 presents a comparison of the sedimentation patterns observed in the experiments (with the laboratory channel dimensions in centimeters and scale numbers in millimeters). As shown in Table 5, the average sedimentation thickness was determined by averaging measurements from 140 points. The volume of eroded material was calculated using Surfer software, and the average sediment mass was obtained by multiplying the eroded material volume by the sediment density.

In the first experiment, the average sediment thickness was 17.2 mm, the eroded material volume was 0.069 m³, and the sediment mass was 99.8 kg. This data allows for the determination of the volume and mass of sediment based on the sedimentation pattern. Additionally, it was observed that the sediment thickness decreases as one moves downstream.

In comparison, the sedimentation-related values in the second experiment were higher than those in the first experiment, indicating the influence of the reservoir sediment movement. Measurements taken after the second experiment showed that approximately 10% of the reservoir sediment had moved downstream. During the second experiment, after the breach of the impermeable core in the development stage, a muddy flow was observed. The majority of the sediment was observed up to one meter downstream of the toe, with a brown sediment layer visible on significant portions of the downstream sedimentation pattern.

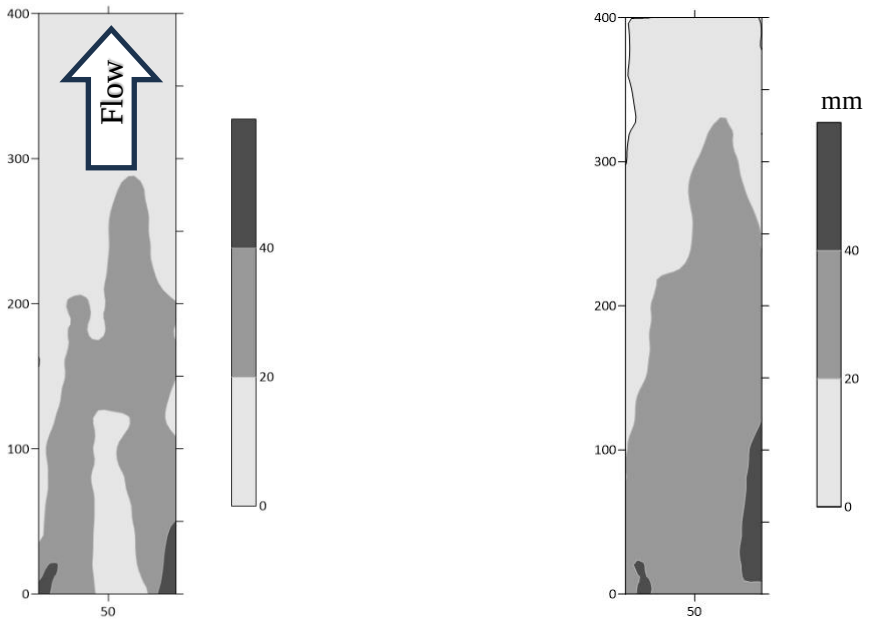

Figure 15. A comparison of sedimentation patterns after dam breach in two experiments: a) The 1st experiment, b) The 2nd experiment

Table 5. Sedimentation patterns results

Subject	Average sedimentation thickness (mm)	Eroded Material volume (m^3)	Sediment mass (kg)
The 1st experiment	17.2	0.069	99.8
The 2nd experiment	23.2	0.093	134.6

4. Conclusion

Based on the experiments conducted and their subsequent analysis, the following results can be summarized:

In the first experiment, three distinct stages were observed, with the breach of the impermeable core marking the transition between the initiation and development stages. During the initiation stage, a 6% increase in the reservoir water level was noted. In the development stage, the rate of change in the reservoir water level was twice that of the final stage. Additionally, the variation rate of the downstream sedimentary flow level was higher than in the other two stages. The maximum downstream flow levels and the formation of the major part of the sedimentation pattern occurred during the development stage.

In the second experiment, a noticeable increase in the average sediment thickness was observed when analyzing the sedimentation pattern. Furthermore, both the volume and mass of the eroded material increased by the end of the experiment, demonstrating the significant impact of reservoir sediment movement. The majority of the transported material was found within one meter downstream of the physical model. By measuring the remaining sediment thickness in the reservoir after the second experiment, it was determined that approximately 10% of the reservoir sediment had moved downstream.

These findings are valuable for mitigating the detrimental effects on downstream regions caused by the breach of embankment dams.

References

1. https://www.icoldchile.cl/boletines/188.pdf
2. https://damsafety.org.
3. Morris, M., & Hassan, M. (2005). IMPACT: Investigation of extreme flood processes and uncertainty-a European research project.
4. Pugh, C. A. (2008). Sediment transport scaling for physical models. In Sedimentation engineering: Processes, measurements, modeling, and practice (pp. 1057-1065).
5. Hanson, G. J., Wahl, T., Temple, D., Hunt, S., & Tejral, R. (2010). Erodibility characteristics of embankment materials. Paper presented at the Proc., ASDSO 2010 Annual Conf., Agriculture Research Service, US Dept. of Agriculture, Washington, DC.
6. Al-Riffai, M. (2014). Experimental study of breach mechanics in overtopped noncohesive earthen embankments. Université d'Ottawa/University of Ottawa.
7. Froehlich, D. C. (2016). Predicting peak discharge from gradually breached embankment dam. Journal of Hydrologic Engineering, 21(11), 04016041.
8. Mohamed, M. M. A., & El-Ghorab, E. A. S. (2016). Investigating scale effects on breach evolution of overtopped sand embankments. Water Science, 30(2), 84-95.
9. Msadala, V. P. (2016). Sediment transport dynamics in dam-break modelling. Stellenbosch: Stellenbosch University.
10. Saberi, O. (2016). Embankment dam failure outflow hydrograph development. Graz University of Technology.
11. https://www.energiforsk.se
12. Sadeghi, S., Hakimzadeh, H., & Babaeian Amini, A. (2020). Experimental investigation into outflow hydrographs of nonhomogeneous earth dam breaching due to overtopping. Journal of Hydraulic Engineering, 146(1), 04019049.

13. Desta, H., & Belayneh, M. (2021). Dam breach analysis: a case of Gidabo dam, Southern Ethiopia. International Journal of Environmental Science and Technology, 18(1), 107-122.
14. Ahadiyan, J., Bahmanpouri, F., Adeli, A., Gualtieri, C., & Khoshkonesh, A. (2022). Riprap effect on hydraulic fracturing process of cohesive and non-cohesive protective levees. Water Resources Management, 36(2), 625-639.
15. Taskaya, E., Bombar, G., & Tayfur, G. (2023). Experimental investigation of sediment movement as a result of homogeneous earth-fill dam overtopping break over a simplified urban area. Journal of Hydrology, 617, 128924.
16. Gee, G. W., & Or, D. (2002). 2.4 Particle-size analysis. Methods of soil analysis: Part 4 physical methods, 5, 255-293.
17. Standard, A. (2007). D698. Standard Test Methods for Laboratory Compaction Characteristics of Soil Using Standard Effort. ASTM International, West Conshohocken, PA.
18. ASTM D 3080 (2004) Standard test method for direct shear test of soils under consolidated drained conditions. American Society for Testing and Materials, W.C.
19. Brontowiyono, W., Hammid, A. T., Jebur, Y. M., Al-Sudani, A. Q., Mutlak, D. A., & Parvan, M. (2022). Reduction of seepage risks by investigation into different lengths and positions for cutoff wall and horizontal drainage (Case study: Sattarkhan Dam). Advances in Civil Engineering, 2022(1), 6441646.
20. USACE, G. D. (2004). Construction Considerations for Earth and Rock-Fill Dams. US Army Corps of Engineers.
21. Reclamation, U. B. O. (1987). Design of small dams. Water Resources Technical Publication, 860p.